ENHANCING THE AUTOMATIC VERIFICATION OF CROPLAND IN HIGH-RESOLUTION SATELLITE IMAGERY

P. Helmholz[a,b]*, F. Rottensteiner[b], C. Fraser[b]

[a]Institute of Photogrammetry and Geoinformation, Leibnitz University Hannover, Nienburger Straße 1,
D-30167 Hannover, Germany - helmholz@ipi.uni-hannover.de
[b]Cooperative Research Centre for Spatial Information, Dept. of Geomatics, University of Melbourne,
723 Swanston Street, Carlton VIC 3053, Australia - (petrah, franzr, c.fraser)@unimelb.edu.au

Commission IV, WG IV/3

ABSTRACT:

Segmentation is one of the first steps in the field of image analyzing and image understanding. It is the basis for the interpretation of images, or it supports other techniques which is the motivation for the in this paper introduced segmentation algorithm. In this paper, a segmentation algorithm and its application to enhance an approach for the automatic verification of tilled cropland objects in a GIS. For this application, cropland objects in a GIS that may contain more than one field should be segmented into individual management units. The algorithm starts with a Watershed segmentation that results in a strong over-segmentation of the image. A region adjacency graph is generated, and neighbouring segments are merged based on similarity of grey levels, noise levels, and the significance of the boundary between the segments. After segmentation, the verification algorithm can be applied separately to the individual segments, and finally, these verification results have to be combined, taking into consideration the specifications of the GIS. Several examples show how the segmentation process can help to improve the verification of the cropland objects in the GIS from IKONOS images covering a test area in Germany, but also the limitations of the segmentation algorithm.

1. INTRODUCTION

The goal of the project WiPKA-QS (Wissensbasierter Photogrammetrisch-Kartographischer Arbeitsplatz – Qualtitätssicherung; Knowledge-based photogrammetric-cartographic workstation – Quality control) is the automatic verification of ATKIS (Amtlich topographisch-kartographisches Informatisonssystem – Authoritative Topographic-Cartographic Information System) or other comparable Geographic Information Systems (GIS) by comparing the GIS with high resolution satellite imagery (Busch et al, 2004). The main components of ATKIS are the object-based digital landscape models with a geometrical accuracy of up to ±3 m.

In order to achieve this goal, a series of algorithms is being developed, each aiming at the verification of a specific object class defined in the GIS. One of the object classes of interest in this context is the class cropland. In Helmholz et al. (2007) an algorithm was introduced to verify tilled cropland objects using characteristic structural features (parallel straight lines) that are generated by agricultural machines during the cultivation. These features are observable in satellite images having a resolution of 1 m or better. The approach works in three steps. For any particular object of class cropland in the GIS, edges are detected in the image area enclosed by the boundary polygon of the object. Then, the edge image is transformed into the Hough space. Finally, after the determination of points of interest (POI) in Hough space, a histogram is calculated. The histogram represents the number of occurrences of POIs in Hough Space (equivalent to lines of interest in the image space) depending on the angle. If a significant orientation is determinate by a statistical analysis of the histogram, the cropland object is accepted. Otherwise, the cropland object is rejected by the system and highlighted as an object that has possibly changed in its land cover or use. The highlighted objects are to be checked by a human operator.

One specification of ATKIS is that inside a cropland object the existence of more than one land cover class is tolerated if a size threshold is not exceeded. Several fields of the same land cover type (different management units) are also permitted inside a cropland object. The existence of more than one management unit negatively affects the edge detection process due to strong differences of the image properties in the different management units. As a consequence, the approach for the detection of parallel lines often fails on GIS objects that contain more than one management unit (Figure 1).

In order to overcome these problems it is necessary to split the cropland object in the GIS into segments having homogeneous grey level properties before carrying out the actual verification process. The individual segments are likely to correspond to different management units provided they have a certain minimum size in object space. After the segmentation, the verification algorithm can be applied independently to the individual management units, which makes it more robust with respect to the automatic tuning of parameters. Afterwards, the verification results of all segments are merged and a final assessment of the GIS object is done; in addition, due to the fact that an individual classification of the homogeneous segments has been carried out, the areas of possible change (i.e., segments found no longer to be cropland objects) can also be highlighted.
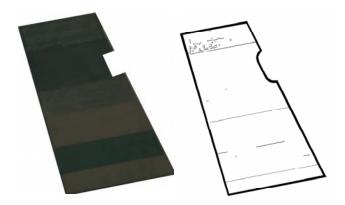
---

* Corresponding author.

Figure 1. Left: A cropland object in Weiterstadt (Germany) in an orthorectified RGB IKONOS image with a resolution of 1 m (acquired 24/06/2003). Right: the edge image as a first step of the verification algorithm.

It is the goal of this paper to present such a segmentation algorithm and first examples for how it can be used to improve the overall verification process. We start with a description of the segmentation algorithm. After that, the way the segmentation algorithm can be embedded into the verification process will be presented. This is followed by preliminary results achieved for images of different resolution and from different locations, which will be the basis for a discussion of the possibilities and the limitations of the segmentation algorithm for this specific application. The paper concludes with a summary and an outlook.

2. REGION-BASED SEGMENTATION

The segmentation of objects provides the basis for the interpretation of images for humans as well as for the fields of Image Analysis and Computer Vision. Compared to the human ability to segment objects directly from an image without great effort, the automatic extraction of objects in the field of image analyzing is difficult due to problems such as variable lighting conditions, poor contrast and the presence of noise. Whereas many segmentation approaches have been presented in the past (e.g. Gonzalez and Woods, 2002; Förstner, 1994), there is no generally accepted optimal approach for segmentation, especially if homogeneous regions are to be extracted. One the one hand, the extracted segments should represent the digital image as precisely as possible, even showing relatively small detectable features; on the other hand, a certain generalisation is required in order to reduce the impact of noise on the segmentation results. Furthermore, segmentation should only be based on a small number of control parameters that should be easily interpretable.

The algorithm presented in this section starts with a Watershed segmentation (Gonzalez and Woods, 2002) that achieves a strong over-segmentation of the image. After that, neighbouring segments are merged on the basis of a statistical analysis of the properties of the initial segments and their shared boundary. The merging process should only require the setting of few control parameters and no training. In that regard it differs from existing grouping algorithms. For instance, Luo and Guo (2003) introduced a general grouping algorithm based on Markov random fields, using single segment properties such as area, convexity and colour variances, and pair-wise properties such as colour differences and edge strength along the shared boundary. The algorithm requires a training phase. Grote et al.

(2007) used mean colour difference, edge strength of the shared borders and colour standard deviation to merge segments of road objects in an iterative way after generating an over segmented image using the Normalized Cut algorithm. Their algorithm requires a priori knowledge given by a GIS and the setting of several thresholds.

2.1 General Segmentation Approach

Let a multispectral image of *N* bands be represented by the grey level vectors $g(x, y) = [g_1(x, y), g_2(x, y), ..., g_N(x, y)]^T$ at position *(x, y)*. It is the goal of region-based segmentation to partition that image into disjunct regions R_i of homogeneous grey level vectors and to determine the closed boundary polygons of these regions. Whereas in theory the boundaries separating these regions are infinitely thin, the reality of the imaging process will blur these boundaries, so that they have actually a certain extent in image space. Typically the region boundaries correspond to edges in the image that can be approximated by polygons. Förstner (1994) represents an image as the union of *segment regions* R_i, *line regions* L_i, and *point regions* P_i, based on a classification of each pixel of the images as being either *homogeneous*, *linear*, or *point-like*. In Fuchs (1998), the symbolic representation was expanded by the neighbourhood relations of these regions to define a *Feature Adjacency Graph* (FAG). In order to distinguish homogeneous pixels from other pixels, a measure for homogeneity *H* can be used that is based on an analysis of the first derivatives of the grey values in a local neighbourhood (Förstner, 1994):

$$H = \sum_{i=1}^{N} \frac{G_\sigma * \left(\Delta g_{ix}^2 + \Delta g_{iy}^2\right)}{\sigma_{ni}'^2} \qquad (1)$$

In Equation 1, g_{ix} and g_{iy} are the first derivatives of the grey levels g_i of band *i* by *x* and *y*, respectively. *G* is a Gaussian smoothing filter with scale parameter , and $'_{ni}{}^2$ is the variance of the smoothed grey level differences $G * g_{ix}$ and $G * g_{iy}$, which can be derived from an estimate of the noise variance $_{ni}$ of band *i* (Brügelmann and Förstner, 1992) by error propagation. The sum is to be taken over the *N* bands of the digital image. The scale parameter defines the size of the local neighbourhood that is taken into account. By normalising the smoothed grey level differences by their standard deviations, the selection of a threshold H_{max} for *H* to distinguish homogeneous pixels from others can be reduced to the selection of a significance level for a statistical test (Förstner, 1994).

The image regions R_i could be determined as connected components of homogeneous pixels, thus of pixels whose homogeneity measure *H* is smaller than H_{max}. However, small gaps within extracted line regions that occur due to poor local contrast often cause a spilling effect, i.e., the erroneous merging of regions that represent different object parts. Furthermore, it is not straightforward to obtain meaningful closed boundary polygons of the homogeneous segments. gives a typical result. The main edges of the image are represented well, although the edges information appears to be captured incompletely. The segments in the label image do not represent the image structure well due to small gaps in their boundaries. A considerable portion of the image is not assigned to any label.

This problem can be overcome by Watershed segmentation, which often produces more stable segmentation results and continuous segment boundaries (Gonzalez and Woods, 2002). Watershed segmentation is based on the interpretation of a digital image as a topographic surface, with the grey values representing heights; the segmentation tries to determine image regions as the catchment areas of local image minima. The boundaries of these regions correspond to watersheds in the topographic surface. For a segmentation that delivers regions of homogeneous grey values, the actual watershed segmentation has to be applied to a gradient image, which has to be smoothed to achieve stable results (Gonzalez and Woods, 2002). As a matter of fact, an image representing the homogeneity value H as defined in Equation 1 can be used as the basis for segmentation, with the parameter   of the Gaussian kernel defining the degree of smoothing.

a)   b)

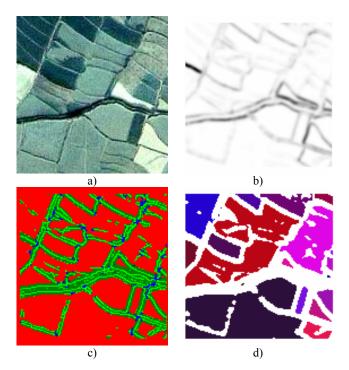c)   d)

Figure 2. a) IKONOS RGB image of Bhutan with a resolution of 1 m; b) Homogeneity image H (inverted for readability), using   = 1. c) Results of classification: homogeneous (red), edge (green); point-like (blue). d): Connected components of homogeneous pixels.

Figure 3 shows the results achieved for a watershed segmentation of the image in Figure 2a using two different smoothing parameters   . In both cases the advantage of watershed segmentation is obvious: it delivers segments with closed and relatively smooth boundaries. However, the left image shows a gross over-segmentation. The segment boundaries a human operator would choose are all there, but there are too many segments. On the other hand, in the segmentation on the right some important image structures have been merged due to the smoothing of the homogeneity image. In order to overcome these problems, we propose an iterative segmentation strategy. First, watershed segmentation is applied with a low degree of smoothing, which results in a strong over-segmentation. Second, a region adjacency graph is generated, which represents the image on a symbolic level and also contains important attributes both of the image segments and

their boundaries. Third, neighbouring regions are merged based on a similarity of attributes and the significance of their separation.

2.2   Region Adjacency Graph

After the initial watershed segmentation, a *Region Adjacency Graph (RAG)* is generated. The nodes of the RAG are the homogeneous segments, whereas its edges represent the neighbourhood relations: two segments S_i and S_j with $i \neq j$ are connected by an edge e_{ij} in the RAG if there is at least one boundary pixel in the segmentation that is neighbour both to S_i and to S_j.
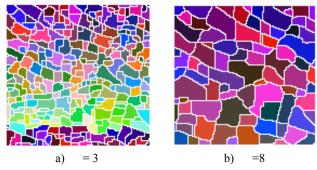

a)   = 3   b)   =8

Figure 3. Watershed segmentation of the image in Figure 2a based on the homogeneity image H (Equation 1) for two values of the smoothing scale   .

When the RAG is constructed, the attributes of both its nodes (the segments) and its edges are determined. A segment S_i has both geometric attributes, namely the number of pixels assigned to the segment, the minimum and maximum coordinates, and the centre of gravity of the segment, and radiometric attributes, namely the average grey level vector $\mathbf{g}^i_{avg} = \mathbf{E}(\mathbf{g}^i)$ and the covariance matrix $\mathbf{Q}^i_{gg}$ of the grey levels. Finally, an overall measure var^i of the noise level inside the segment is determined as the trace of $\mathbf{Q}^i_{gg}$: $var^i = trace(\mathbf{Q}^i_{gg})$. In order to make the computation of $\mathbf{g}^i_{avg}$ and $\mathbf{Q}^i_{gg}$ robust with respect to outliers next to the segment boundary, grey level vectors that are close to the segment boundary are excluded from the computation. However, all grey level vectors are used for the computation if a segment is so small that all its pixels are within such a distance from its boundary that they would thus be excluded.

An edge e_{ij} in the RAG represents a neighbourhood relation between two segments S_i and S_j and, thus, also the boundary between these regions. Note that the boundary between two segments may consist of one or more sequences of boundary pixels. That is why each edge in the RAG contains a set of connected boundary pixel chains that are extracted from the label image representing the segmentation results. Furthermore, the boundary pixels have a 2D extent in the digital image, i.e. the area covered by these pixels. Thus, an edge e_{ij} also has an average grey level vector and a covariance matrix of grey levels, computed from the grey levels of all the boundary pixels separating S_i and S_j. Finally, a measure T_{ij} for the strength of the boundary is determined as the percentage of boundary pixels for which the homogeneity measure H (Equation 1) is larger than the threshold H_{max} that would be used for edge extraction. In this context, it is advisable to re-compute H using a relatively small value for the smoothing parameter   , e.g.   = 0.7. T_{ij} can be interpreted as the percentage of edge pixels contained in the boundary separating the two segments S_i and S_j. It will be

large if the boundary corresponds to an image edge and thus to a real grey level discontinuity, whereas it will be small for edges that separate two segments of a similar distribution of grey values.

2.3 Merging of Regions Having Similar Attributes

The RAG and the attributes of both its nodes and its edges are the basis for merging neighbouring regions to improve the initial segmentation. It is the goal of this process to merge regions that have similar radiometric properties and noise levels, but that are not separated by a significant edge. First, a distance metric D_{ij} is computed for each edge e_{ij}:

$$D_{ij} = \frac{\left(\mathbf{g}^i_{avg} - \mathbf{g}^j_{avg}\right)^T \cdot \left(\mathbf{Q}^i_{gg} + \mathbf{Q}^j_{gg}\right)^{-1} \cdot \left(\mathbf{g}^i_{avg} - \mathbf{g}^j_{avg}\right)}{\chi^2_{N,1-\alpha}} \qquad (2)$$

In Equation 2, the vector $\mathbf{g}^i_{avg} - \mathbf{g}^i_{avg}$ is the difference vector between the average grey level vectors of the two regions, and $\chi^2_{N,1-}$ is the $1-$ quantile of a chi-square distribution with N degrees of freedom, where N is the number of image. Two regions S_i and S_j are said to have similar attributes if the value of D_{ij} is smaller than 1. This corresponds to a statistical test whether the difference between two grey level vectors having the covariance matrices $\mathbf{Q}^i_{gg}$ and $\mathbf{Q}^j_{gg}$ is significant, though it is not a test whether the difference between the average grey level vectors is significant. In any case, the selection of a threshold for the difference between grey level vectors is replaced by selecting a significance level .

However, the distance metric D_{ij} is not the only indicator used for identifying similar homogeneous regions. D_{ij} is small if the difference between the average grey level vectors is small or if the variances of the grey levels inside a region are large. This means that if one image segment is highly textured (e.g. because it contains trees), it might be merged with neighbouring segments that are quite homogeneous, because the grey level difference can be statistically explained by the variances of the grey levels in the highly textured segment. Thus, we restrict the set of regions that can be merged to those having a similar level of noise. We introduce a second metric, the variance factor F^v_{ij} that compares the two noise levels var^i and var^j of S_i and S_j:

$$F^v_{ij} = \frac{1}{F_{N \cdot Pi_i, N \cdot Pj, 1-\alpha}} \cdot \frac{var^i}{var^j} \qquad (3)$$

In Equation 3, it is assumed that $var^i > var^j$; $F_{N \cdot Pi, N \cdot Pj, 1-}$ is the $1-$ quantile of a Fisher distribution with $N \cdot Pi$ and $N \cdot Pj$ degrees of freedom, where N is the number of image bands and Pi and Pj are the numbers of pixels assigned to S_i and S_j. The segments may only be merged if F^v_{ij} is smaller than a threshold. Using a value of 1 for that threshold corresponds to a statistical test for the identity of the two noise levels.

Finally, even if two segments have similar grey level distributions and a similar noise level, they still might be separated by a significant edge, e.g. by a small path between two fields, as it is the case in the upper corner in Figure 2a. As stated above, an edge in the RAG contains the vector of average grey levels and the covariance matrix of the grey levels of the

boundary between the two neighbouring segments and a measure T_{ij} for the strength of the boundary. Two segments may only be merged if the distance metric according to Equation 1 between the merged segment and the boundary region is smaller than 1 and if T_{ij} is smaller than 0.5, i.e. if less than 50% of the pixels separating S_i and S_j are edge pixels.

Thus, by applying the rules described in this section, a set of tuples of regions S_i and S_j that may be merged can be constructed. This set is ordered by the distance metrics D_{ij}; the first element thus corresponds to the two segments having the most similar grey level distributions while still having a similar noise level and not being separated by a significant edge. These segments are merged, including the boundary pixels that formerly separated them, and the RAG is updated. In this context, the segment label image has to be changed, the attributes of the new merged segment have to be determined, and the edges of the RAG have to be updated. This analysis is repeated iteratively until no more segments can be merged. Figure 4 shows the segment label image generated by grouping the original labels in Figure 3a.
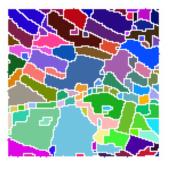

Figure 4. Segment label image generated by grouping the original labels in Figure 3a.

3. USING THE SEGMENTATION ALGORITHM FOR THE VERIFICATION OF CROPLAND

The segmentation algorithm presented in the previous section was implemented in the software system BARISTA (Barista, 2008). In this section we will describe its integration into the WiPKA-QS verification process for cropland objects. We will show the individual stages of the process using the image shown in Figure 1 as an example. Figure 5a shows the initial segmentation of that image after Watershed segmentation using a smoothing scale of . = 1. Figure 5b shows the results of the merging process described in Section 2.

The results shown in Figure 5b are not perfect. The main management units have been separated correctly, but there remains some noise in the form of small insular segments and especially at the region boundaries. As mentioned in section 1, several objects of the same land cover type are permitted inside an ATKIS cropland object, and the existence of small areas having a different land cover class is tolerated if a size threshold is not exceeded and if the actual land cover is similar to cropland (e.g. grassland). These definitions can be used to further improve the segmentation in Figure 5b. Regions that are surrounded by just one other region and are smaller than a given area threshold are merged with the surrounding segment. Figure 6 shows the results of merging small insular regions smaller than 1000 m[2] with their surrounding larger segments.

The segmentation results in Figure 6 represent the real cropland segments in the GIS object much better than those in Figure 5b. Most of the small disturbances could be eliminated. In the uppermost segment there are still a lot of disturbances caused by rows of trees that indicate a land use as a small orchard (class *special cultures* in ATKIS). Despite being small, these objects were not merged with their surrounding segments because they were bordered by more than one segment. In an ATKIS cropland object, *special cultures* objects are permitted as long as they not exceed a size threshold. For this reason it is important for the application not to merge such non-cropland objects with their surrounding cropland areas, because otherwise the next analysis step might reject the larger segment as a cropland object even though it is consistent with ATKIS specifications for that class.
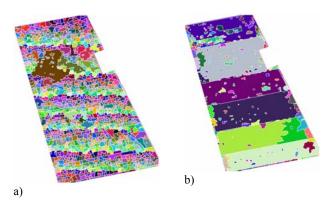

a)

b)

Figure 5. a) Watershed segmentation of the image in Figure 1 using a smoothing scale of . = 1. b) Segmentation results after region merging.
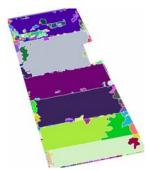

Figure 6. Segmentation results after removing segments having only one neighbour and being smaller than 1000 m^2.

Other disturbances are located near the object border due to a changing tilling direction. These structures caused by turning agricultural machines would disturb the verification algorithm and are thus excluded from the analysis of the predominant edge direction (Helmholz et al., 2007). For that reason, the segmentation can also be restricted not to consider areas close to the object boundaries. An example for the influence of this restriction on the segmentation results is shown in Figure 7.

Most of the disturbances close to the object boundary could be eliminated. The few remaining ones have no influence on the next analysis step due to their small size. Of course, the small segments corresponding to the orchard in the uppermost part of the GIS object remain. The two management units at the lower end of the GIS object are both split into two parts. This is caused by slightly different reflectance properties of these areas

due to different soil characteristics. However, all of these segments are large enough for the verification step to detect a sufficient number of parallel lines for success.

The label image in Figure 7 is the basis for the analysis of parallel lines that is used for the verification of the original cropland object. The verification algorithm is applied to each of the segments in Figure 7 exceeding a certain size rather than to the whole area corresponding to the ATKIS cropland object. After that the individual results of verification are merged in a final analysis step taking into account the definitions of ATKIS for the representation of cropland objects. Compared to the original algorithm (Helmholz et al., 2007) this is expected to lead to better results because the smaller segments should be more uniform in their main tilling direction.

Figure 7. Results of segmentation if regions near to the object border are not considered.

Figure 8 and Figure 9 show two more examples for ATKIS cropland objects that are taken from the same IKONOS scene as Figure 1. Note that the ATKIS cropland object Figure 8 consists of only one management unit, whereas both in Figure 1 and in Figure 9 there are multiple units. It is obvious that the segmentation algorithm detects homogeneous image regions that do not necessarily coincide with management units, because the algorithm is affected by characteristics of the soil such as humidity or soil material. Typical examples are the field at the bottom of Figure 7, the area in the left of the field in Figure 8, and the field in the middle of Figure 9. The different reflectance properties of the soil are the main reason for remaining small disturbances. The number of these disturbances is of course higher when the smoothness parameter of the Watershed algorithm is lower (compare Figure 8b and c). If a field is thus split into segments that are large enough for the following analysis to succeed (bottom management unit in Figure 7), the appearance of different soil characteristic has no influence on the application. This is also true if the major part of a segment is correctly extracted and the remaining disturbances are small enough to be disregarded in the following analysis (the management units in the middle of Figure 7). However, the management unit in the middle of Figure 9 is split into too many small segments, which would prevent the verification algorithm from correctly classifying that region. Also the large segment in the left part of Figure 8c would not be verified correctly despite being too large for being discarded: no parallel straight lines are detected (cf. Figure 8d). However, in the case Figure 8c, the largest part of the ATKIS object would be verified correctly. The distance metric between the large segment and the disturbing object suggests that they could be merged, but the measure T_{ij} for the strength of the boundary between them prevents the algorithm from merging them. It might be possible to consider this when the classification results of the individual are merged: if an object that could not be verified is surrounded entirely by a verified

object of similar reflectance properties, it could be considered as verified, too, despite the absence of the structural indicators. Another idea to enhance the segmentation results is to use a priori knowledge about the typical shape of management units to introduce additional constraints. Using the information that the boundaries of management units usually consist of straight line segments that are orthogonal or nearly orthogonal could improve the results for the examples given in Figure 7 and Figure 8. Unfortunately, these geometrical constraints could hardly improve the segmentation result in Figure 9.
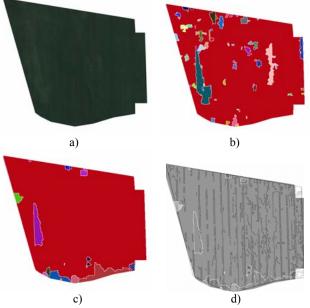

Figure 8. a) Original image, taken from the same IKONOS scene as Figure 1a; b) Results of segmentation (smoothness for Watershed = 1); c) Results of segmentation (smoothness for Watershed = 5); d) white lines: segment boundaries from c), black lines: results of edge detection.
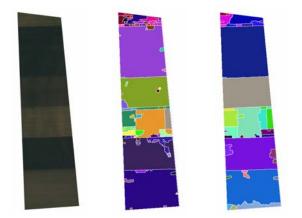

Figure 9. RGB IKONOS image (left); grouping result with smoothness for watershed = 1 (middle); grouping result with smoothness for watershed = 5 (right)

4. CONCLUSIONS AND OUTLOOK

The goal of the presented segmentation algorithm was the enhancement of an algorithm for the verification of tilled cropland objects by splitting that object into homogenous regions. This is necessary because the verification algorithm does not work successfully with GIS objects containing more than one management unit. Despite disturbances caused by

variations of the soil properties, the homogenous regions are to a large degree coherent with the different management units existing in a GIS object. The segmentation algorithm is still work in progress, but the preliminary results presented in this paper show the potential of the algorithm for the verification approach. Even though a complete segmentation of management units seems to be impossible, the segmentation algorithm enhances the automatic verification process of GIS object. The level of segmentation that could achieved is already an important improvement of the verification approach.

Future work comprises an improvement of the segmentation algorithm, e.g. by introducing additional (geometrical) constraints, and the implementation of the synthesis of the verification results achieved for the individual segments: at this instance, segmentation errors could be compensated. Furthermore, a more detailed evaluation of the improvement achieved by the segmentation is to be carried out.

REFERENCES

Barista, 2008. Barista product information webpage, *http://www.baristasoftware.com.au* (Accessed: 30. April 2008).

Brügelmann, R., Förstner, W., 1992. Noise estimation for color edge extraction. In: *Robust Computer Vision*, Wichmann, Karlsruhe (Germany), pp. 90-107.

Busch, A., Gerke, M., Grünreich, D., Heipke, C., Liedtke, C.-E., Müller, S., 2004. Automated verification of a topographic reference dataset: system design and practical results. International Archives of Photogrammetry & Remote Sensing XXXV-B2, pp. 735-740.

Förstner, W., 1994. A framework for low level feature extraction. Computer Vision - ECCV '94. Proc. 5th ICCV, vol. II, pp. 383-394.

Fuchs, C., 1998: Extraktion polymorpher Bildstrukturen und ihre topologische und geometrische Gruppierung. PhD Thesis, Institute of Photogrammetry, Bonn University, DGK-C 502.

Gonzalez, R., Woods, E., 2002. *Digital Image Processing*. 2nd edition, Prentice Hall, Upper Saddle River (NJ), pp. 622-624.

Grote, A., Butenuth, M., Heipke, C., 2007. Road extraction in suburban areas based on Normalized Cuts. International Archives of Photogrammetry, Remote Sensing and Spatial Information Sciences, 36(3/W49A), pp. 51-56.

Helmholz, P., Gerke, M., Heipke, C., 2007. Automatic discrimination of farmland types using IKONOS imagery. International Archives of Photogrammetry, Remote Sensing and Spatial Information Sciences, 36(3/W49A), pp. 81-86.

Luo, J., Guo, C., 2003. Perceptual grouping of segmented regions in color images. Pattern Recognition 36(2003):2781-2792.